

# Energetics and Electronic Structure of Plutonium

Nicola Lanatà,<sup>1,\*</sup> Yong-Xin Yao,<sup>2,\*</sup> Cai-Zhuang Wang,<sup>2</sup> Kai-Ming Ho,<sup>2</sup> and Gabriel Kotliar<sup>1</sup>

<sup>1</sup>*Department of Physics and Astronomy, Rutgers University, Piscataway, New Jersey 08856-8019, USA*

<sup>2</sup>*Ames Laboratory-U.S. DOE and Department of Physics and Astronomy, Iowa State University, Ames, Iowa IA 50011, USA*

(Dated: June 23, 2021)

Plutonium is the most exotic and mysterious element in the periodic table. It has 6 metallic phases and peculiar physical properties not yet understood. One of the most intriguing properties of Pu is that relatively small changes of temperature can induce transitions between different structures, that are accompanied by very large changes of equilibrium volumes. This fact has stimulated extensive theoretical and experimental studies. In spite of this, a convincing explanation of the metallurgic properties of Pu based on fundamental principles is still lacking, and none of the previous theories has been able to describe simultaneously the energetics and the  $f$  electronic structure of all of the phases of Pu on the same footing. Here we provide a bird's eye view of Pu by studying the zero-temperature pressure-volume phase diagram and the  $f$  electronic structure of all of its crystalline phases from first principles. In particular, we clarify the way in which the  $f$ -electron correlations determine its unusual energetics. Our theoretical energetics and ground-state  $f$  electronic structure are both in good quantitative agreement with the experiments.

The stable structure of plutonium at ambient conditions is  $\alpha$ -Pu, that has a low-symmetry monoclinic structure with 16 atoms within the unit cell grouped in 8 nonequivalent types. At higher temperatures, see Fig. 1, Pu can assume the following distinct lattice structures:  $\beta$  (monoclinic, with 34 atoms within the unit cell grouped in 7 inequivalent types),  $\gamma$  (orthorhombic),  $\delta$  (fcc),  $\delta'$  (bct), and  $\epsilon$  (bcc). These temperature-induced structure-transitions are accompanied by significant changes of volume, that are still not well understood. In particular, the equilibrium volumes of the  $\delta$  and  $\delta'$  phases are very large with respect to the other allotropes. Another interesting puzzle is that  $\delta$ - and  $\delta'$ -Pu have negative thermal-expansion coefficients within their respective range of stability, unlike the vast majority of materials.

It is clear that a theoretical explanation of the properties of Pu needs to be supported by first-principles calculations which, not only are able to take into account the details of the band-structure and the strong-correlation effects, but are also able to evaluate precisely the total energy. Previous state-of-the-art density functional theory (DFT) calculations [1–4] were able to reproduce the

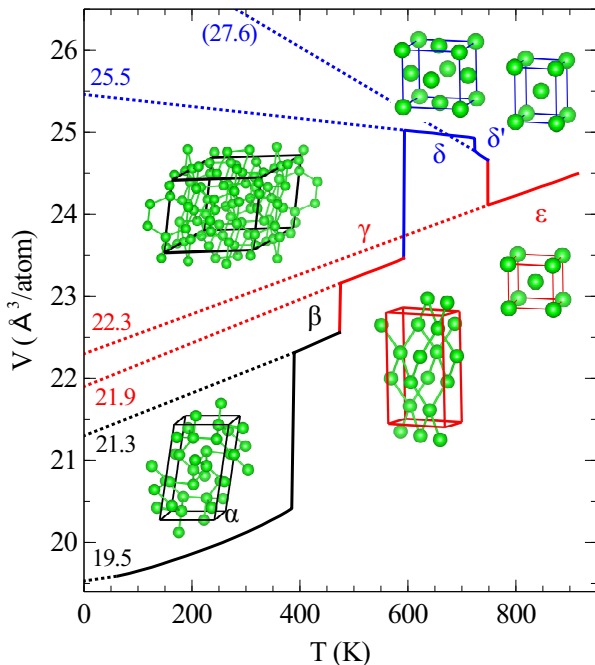


FIG. 1: Experimental volume-temperature phase-diagram of Pu. The dotted lines indicate the zero-temperature equilibrium volumes extrapolated by linear interpolation.

energetics of Pu, but in order to describe all of the phases on the same footing it was necessary to introduce artificial [5] spin and/or orbital polarizations — thus compromising the description of the electronic structure. Calculations within the framework of DFT in combination with dynamical mean field theory (DFT+DMFT) have been able to explain several aspects of the electronic structure of Pu, see, e.g., Refs. [6–9]. Nevertheless, the computational complexity of this approach made it impossible to calculate the pressure-volume phase diagram of all of the phases of Pu. In this work we overcome these issues by using the charge self-consistent combination of the Local Density Approximation and the Gutzwiller Approximation (LDA+GA) [10–14], whose description of the ground-state properties is generally in very good agreement with LDA+DMFT, but is considerably less computationally demanding. In particular, we employ the numerical approach derived in Ref. [15].

In the upper panels of Fig. 2 are shown the LDA (left) and LDA+GA (right) evolutions of the total energies  $\mathcal{E}$

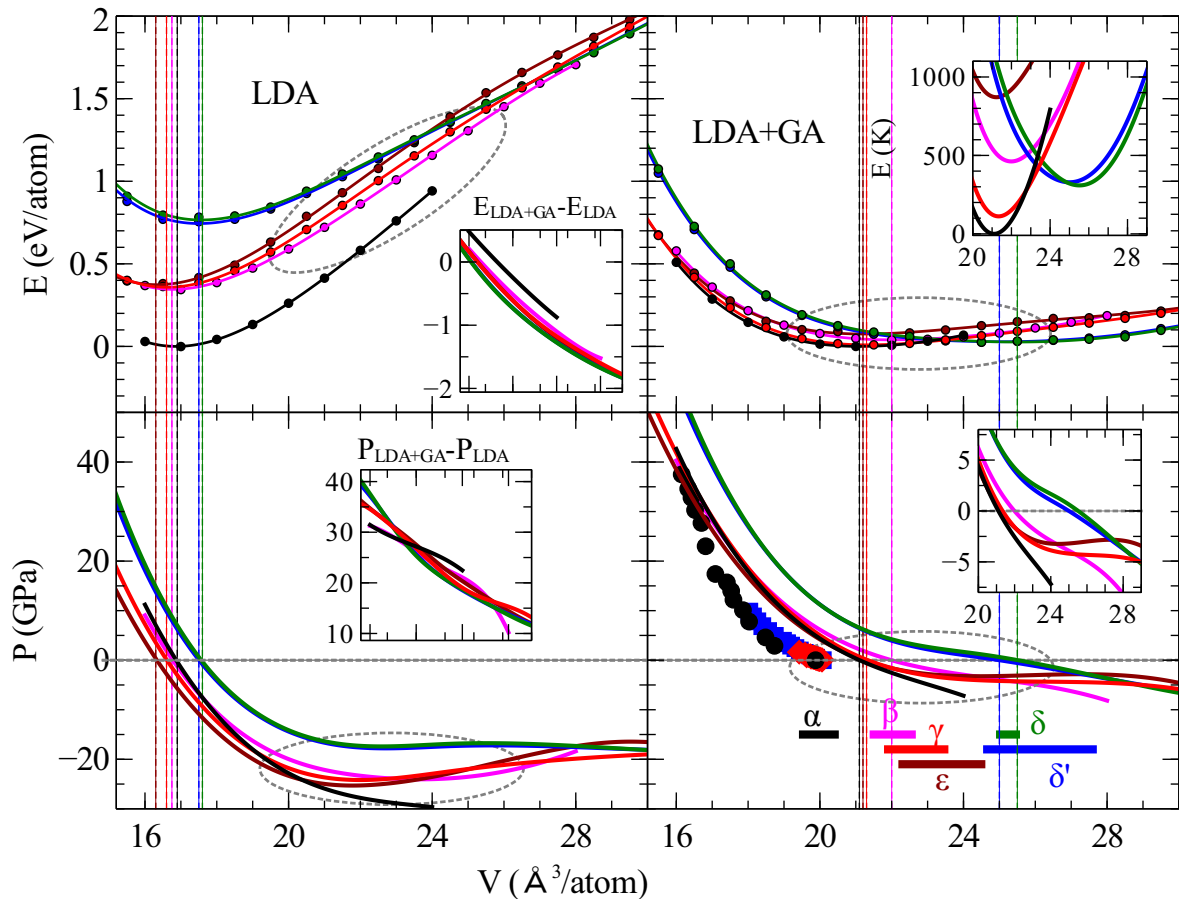


FIG. 2: Theoretical total energies for the crystalline phases of Pu as a function of the volume (upper panels) and corresponding pressure-volume curves (lower panels). Our results are shown both in LDA (left panels) and in LDA+GA (right panels). The right insets are zooms of the curves in the corresponding panels. In the upper-left inset are shown the correlation energies — here defined as the differences between the LDA+GA and LDA total energies, — while the corresponding contributions to the pressure are shown in the lower-left inset. The vertical lines indicate the minima of the energy curves. The lines of the legend indicate the estimated zero-temperature equilibrium volumes. The LDA+GA pressure-volume curves are shown in comparison with the experimental data of  $\alpha$ -Pu from Ref. [16] (black circles), Ref. [17] (blue squares) and Ref. [18] (red diamonds).

TABLE I: Zero-temperature theoretical equilibrium volumes, bulk modulus and total energies of the crystalline phases of Pu in comparison with the experiments [19, 20]. The total energies are relative to the ground-state energy of  $\alpha$ -Pu. The zero-temperature equilibrium volumes of  $\gamma$ - and  $\epsilon$ -Pu are extrapolated by linear interpolation from the experimental data reported in Fig. 1. Note that the experimental value of the  $\delta$ -Pu bulk-modulus refers to the 1.9% Ga alloy.

Pu	$\alpha$	$\beta$	$\gamma$	$\delta$	$\delta'$	$\epsilon$
$V_{\text{exp}} (\text{\AA}^3)$	19.5	21.9	22.3	25.2	25.1	22.3
$V_{\text{th}} \pm 0.5 (\text{\AA}^3)$	21.1	22.0	21.3	25.5	25.0	21.2
$E_{\text{exp}} (K)$	0	470	550	620	710	1130
$E_{\text{th}} \pm 100 (K)$	0	460	110	310	330	870
$K_{\text{exp}} (GPa)$	70.2	—	—	38	—	—
$K_{\text{th}} (GPa)$	50–70	40–55	45–70	15–35	10–25	35–55

as a function of the volume  $V$  for all of the crystalline phases of Pu. In the lower panels are reported the corresponding evolutions of the pressure  $\mathcal{P} = -d\mathcal{E}/dV$  in comparison with the experimental data of  $\alpha$ -Pu. In the left insets are shown the correlation energies — here defined as the differences between the LDA+GA and LDA total energies — and the respective contributions to the pressure. Note that in our calculations we have not performed structure relaxation, but we have assumed a uniform rescaling of the experimental lattice parameters, see Refs. [18, 21].

In table I the theoretical zero-temperature equilibrium volumes are shown in comparison with the zero-temperature experimental volumes, that we assume to be in between the thermal-equilibrium volumes and the zero-temperature values extrapolated by linear interpolation in Fig. 1. The bulk modulus and energies (referred

to the ground-state energy of  $\alpha$ -Pu) are shown in comparison with the experimental data of Refs. [19, 20]. Note that the numerical error for the theoretical bulk modulus is due to the fact our calculations are performed only on a discrete mesh of values, see the upper panels of Fig. 2. Remarkably, while the theoretical equilibrium volumes of all phases of Pu are very similar in LDA, they are very different in LDA+GA, and in good quantitative agreement with the zero-temperature experimental values. Furthermore, while LDA predicts very large equilibrium energy-differences between the phases of Pu, these differences are very small in LDA+GA, in agreement with the experiments. Note also that the LDA+GA ground-state energies increase monotonically from each phase to the next-higher-temperature phase, consistently with the experiments, see Fig. 1 and Table I. The only exception is  $\beta$ -Pu, whose theoretical equilibrium energy is larger than  $\gamma$ -,  $\delta$ - and  $\delta'$ -Pu.

In order to understand how the electron-correlations affect so drastically the energetics of Pu, it is enlightening to look at the behavior of the correlation energies, see the left insets in Fig. 2. In fact, the evolution of the correlation energies as a function of the volume is essentially structureless and identical for all of the phases (made exception for a uniform structure-dependent energy shift whose main effect is to slightly increase the energy of  $\alpha$ -Pu with respect to the other phases). As a result of this correction, the LDA total energies are transformed in the way indicated by the gray circles in the upper panels of Fig. 2. The relative behavior of the LDA+GA zero-temperature energies of the allotropes of Pu is clearly inherited by the LDA energy-volume curves in the region highlighted in the upper-left panel of Fig. 2, which transform into the region highlighted in the upper-right panel of Fig. 2 when the correlation energies are taken into account. The same considerations apply to the evolutions of the pressure, as indicated by the gray circles in the lower panels of Fig. 2. The above observation explains from a simple perspective how the electron correlations determine the unusual energetics of Pu.

In the upper panels of Fig. 3 are shown the occupations of the  $f$  electrons. The total number of  $f$  electrons in  $\delta$ -Pu is  $n_f \simeq 5.2$ , which is consistent with previous LDA+DMFT calculations [7]. Here we find that  $n_f \simeq 5.2$  also for  $\gamma$ -,  $\delta'$ - and  $\epsilon$ -Pu. In the monoclinic structures  $n_f$  is different for the inequivalent atoms within the unit cell, and it runs between 5.21 and 5.32 in  $\alpha$ -Pu while it runs between 5.17 and 5.21 in  $\beta$ -Pu. In the middle panels of Fig. 3 are shown the averaged orbital populations with total angular momentum  $J = 7/2$  and  $J = 5/2$ . Note that for all of the phases of Pu the number of  $7/2$   $f$  electrons decreases as a function of the volume, while the number of  $5/2$   $f$  electrons increases. This behavior indicates simply that the spin-orbit effect is more effective at larger volumes, as expected. Finally, in the lower panels is shown the behavior of the branching ratio  $B$ , which is

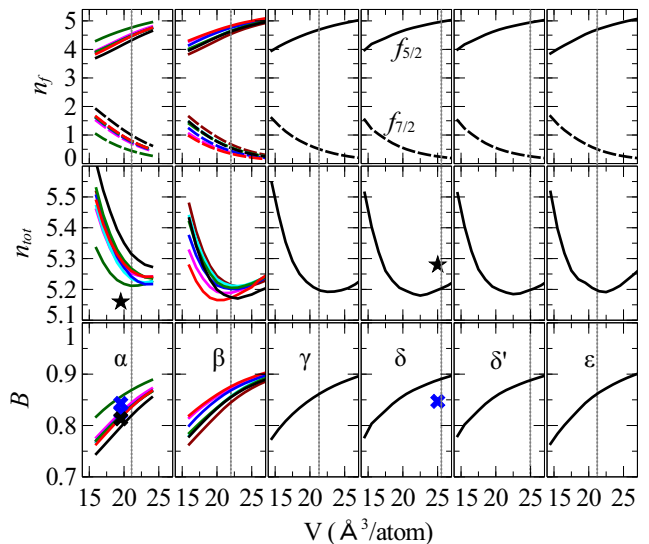


FIG. 3: Upper panels: evolution as a function of the volume of the averaged orbital populations of the  $5/2$  and  $7/2$   $f$  electrons. Middle panels: total orbital occupations in comparison with the values extrapolated in Ref. [22] from XANES measurements at ambient conditions of  $\alpha$ -Pu (black stars) and the 1.9%-Ga  $\delta$ -Pu alloy. Lower panels: theoretical branching ratios in comparison with the values extrapolated in Refs. [23, 24] from XAS (black cross) and EELS (blue crosses) experiments of  $\alpha$ -Pu and the 0.6%-Ga  $\delta$ -Pu alloy. The colors in the first and second panels from the left correspond to the inequivalent atoms of  $\alpha$ -Pu and  $\beta$ -Pu. The vertical dotted lines indicate the LDA+GA equilibrium volumes for the respective phases.

a measure of the strength of the spin-orbit coupling interaction in the  $f$  shell, and is calculated from the orbital populations making use of the equation

$$B = \frac{3}{5} - \frac{4}{15} \frac{1}{14 - n_{5/2} - n_{7/2}} \left( \frac{3}{2} n_{7/2} - 2 n_{5/2} \right), \quad (1)$$

see Ref. [25, 26]. Consistently with the behavior of the orbital populations,  $B$  increases as a function of the volume. Note that the behavior of  $n_f$  and  $B$  is very similar for all of the phases of Pu.

The  $\alpha$ -Pu theoretical value of  $n_f$  at equilibrium is in good agreement with the values extrapolated from the X-ray absorption near-edge structure (XANES) measurements of Ref. 22. On the other hand, while our calculations indicate that  $n_f$  is slightly smaller in  $\delta$ -Pu than in  $\alpha$ -Pu, according to the extrapolations of Ref. 22, the 1.9%-Ga  $\delta$ -Pu alloy has a larger  $n_f$  with respect to  $\alpha$ -Pu. Also the theoretical values of  $B$  are in good agreement with values extrapolated in Refs. [23, 24] from electron energy-loss spectroscopy (EELS) and X-ray absorption spectroscopy (XAS) [27–30].

Let us study the behavior of the many-body reduced density matrix  $\hat{\rho}_f$  of the  $f$  electrons, which is obtained from the full many-body density matrix of the system

by tracing out all of the degrees of freedom with the exception of the  $f$  local many-body configurations of one of the Pu atoms. We define

$$\hat{F} \equiv -\ln \hat{\rho}_f + k, \quad (2)$$

where  $k$  is an arbitrary constant that we determine so that the lowest eigenvalue of  $\hat{F}$  is zero by definition. Within this definition  $\hat{\rho}_f \propto e^{-\hat{F}}$ , i.e.,  $\hat{F}$  represents an effective local Hamiltonian of the  $f$  electrons that depends on the volume, and that is renormalized with respect to the atomic  $f$  Hamiltonian because of the entanglement with the rest of the system, see Ref. [31].

Fig. 4 shows the eigenvalues  $P_n$  of  $\hat{\rho}_f$  as a function of the eigenvalues  $f_n$  of  $\hat{F}$  for all of the allotropes of Pu (that are computed at their respective theoretical zero-temperature equilibrium volumes). Consistently with Ref. [7], we find that for  $\delta$ -Pu there are two dominant groups of multiplets: one with  $N = 5$  and  $J = 5/2$  (that is 6 times degenerate), and one with  $N = 6$  and  $J = 0$  (that is non-degenerate). Interestingly, our results show that this conclusion applies also to all of the other phases. The  $f$  probability distribution of  $\delta$ - and  $\delta'$ -Pu is slightly less broad with respect to the other phases. This is to be expected, as  $\delta$ - and  $\delta'$ -Pu are stable at larger volumes, so that the local  $f$  degrees of freedom are less entangled with the rest of the system with respect to the other phases. The  $f$  probability distributions of  $\alpha$ - and  $\beta$ -Pu are considerably different for inequivalent atoms, as they depend on the number and relative distances of the nearest-neighbor atomic positions, consistently with Refs. [15, 32]. Note that in  $\beta$ -Pu the atom-dependency of the  $f$  probability distribution is less pronounced than in  $\alpha$ -Pu.

We point out that the fact that  $n_f \simeq 5.2$  reveals that the  $f$  electrons of Pu are in a pronounced mixed-valence state [33]. Indeed, the probability of the  $N = 6, J = 0$  multiplet is very large, as indicated by the fact that it has the lowest  $\hat{F}$  eigenvalue. The reason why  $n_f$  is closer to 5 than to 6 is that the  $N = 6, J = 0$  multiplet is non-degenerate, while the  $N = 5, J = 5/2$   $\hat{F}$ -eigenvalue is 6 times degenerate — so that its contribution to  $n_f$  is weighted by a factor  $6 = 2 \times 5/2 + 1$ . The observation that the  $f$  electrons have a significant mixed-valence character indicates that the local  $f$  degrees of freedom are highly entangled with the rest of the system [31]. This observation is consistent with the fact that the Pauli susceptibility of the  $\delta$ -Pu Ga alloy is Pauli-like at low temperatures [5]. Furthermore, it is consistent with the statement of Ref. [20] that Pu is an ordinary quasiharmonic crystal in all of its crystalline phases, i.e., that already at  $T \gtrsim 200$  K the electronic entropy is very small with respect to the quasiharmonic contributions.

In conclusion, in this work we have calculated from first principles the zero-temperature energetics of Pu, finding very good agreement with the experiments. Our analysis

has clarified how the electron correlations determine the unusual energetics of Pu, including the fact that the different allotropes have very large equilibrium-volume differences while they are very close in energy. Remarkably, in our calculations we did not introduce any artificial spin and/or orbital polarizations [5], while this was necessary in previous state-of-the-art DFT calculations [1–4]. This advancement has enabled us to describe also the  $f$  electronic structure of Pu on the same footing. Our calculations indicate that the ground-state  $f$  electronic structure is similar for all phases of Pu, and that the  $f$ -electron atomic probabilities display a significant mixed-valence character. Our zero-temperature calculations of Pu constitute also an important step toward the theoretical understanding of its peculiar temperature-dependent properties, e.g., the negative thermal expansion of  $\delta$ - and  $\delta'$ -Pu. In fact, above room temperature, the contributions to the free energy of the non-adiabatic effects and of the thermal excitations of the electrons from their ground state are expected to be negligible in Pu [20]. Consequently, the ground-state total energy could be used to derive microscopically the atomistic potentials and study from first principles the evolution of the atom positions as a function of the temperature making use of the Born-Oppenheimer approximation.

## METHODS

In this work we have employed the LDA+GA charge self-consistent numerical scheme of Ref. [15]. The interface between Wien2k [34] and the GA has been coded following Ref. [35]. The calculations have been performed making use of the general Slater-Condon parametrization of the on-site interaction, assuming  $U = 4.5$  eV and  $J = 0.36$  eV, consistently with Ref. [15]. We have employed the following standard form for the double-counting functional

$$E_{\text{dc}}^{\text{St}}[n_f] = \frac{U}{2} n_f(n_f - 1) - \frac{J}{2} n_f(n_f/2 - 1), \quad (3)$$

where  $n_f \equiv \langle \Psi | \hat{n}_f | \Psi \rangle$  is the total number of  $f$  electrons.

## CONTRIBUTIONS

N.L. and Y.X.Y. carried out the LDA+GA calculations, analyzed the data, and co-developed the GA code (open source “FastGutz” package) under the supervision of G.K., C.Z.W and K.M.H. . N.L. led the project and wrote the manuscript. Y.X.Y. coded the interface between Wien2k and the GA solver, which was constructed on the basis of the LDA+DMFT interface developed by K.H., and parallelized the GA solver. G.K. proposed the project and supervised the research.



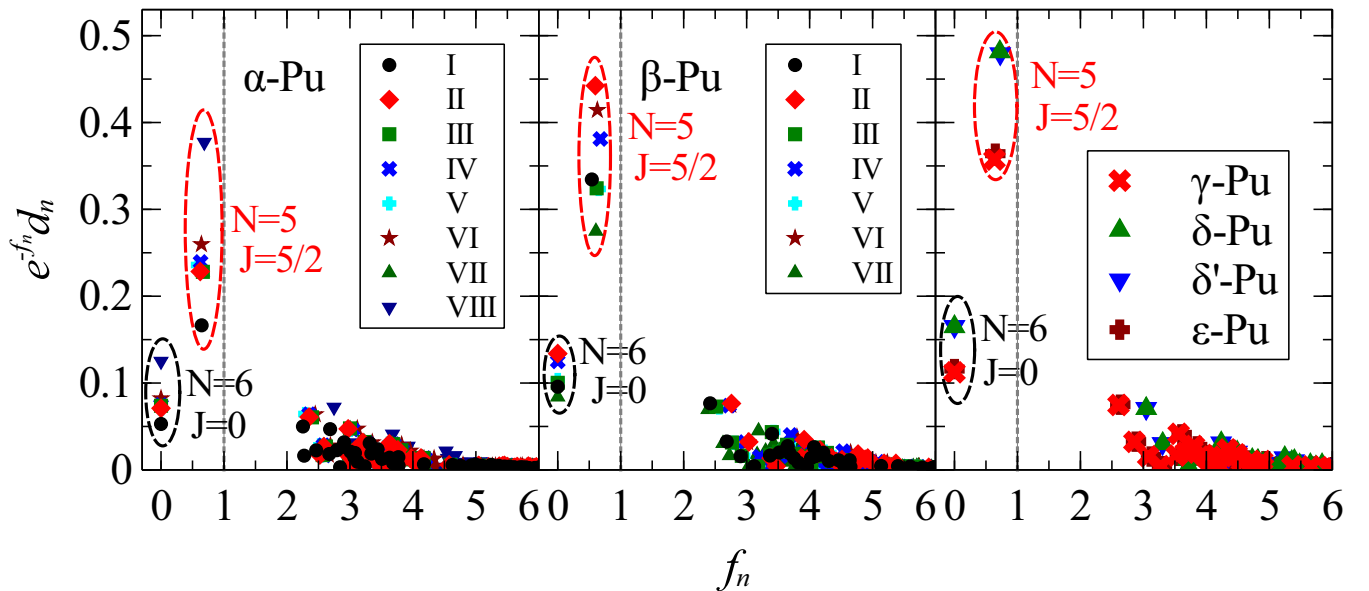


FIG. 4: Configuration probabilities of the eigenstates of the reduced density matrix  $\hat{\rho}_f \equiv e^{-\hat{F}}/\text{Tr}[e^{-\hat{F}}]$  of the  $f$  electrons as a function of the eigenvalues  $f_n$  of  $\hat{F}$ . Each configuration probability is weighted by the degeneracy  $d_n = 2J_n + 1$  of the respective eigenvalue  $f_n$ , where  $J_n$  is the total angular momentum.

#### ACKNOWLEDGMENTS

We thank XiaoYu Deng and Kristjan Haule for useful discussions. N.L. and G.K. were supported by U.S. DOE Office of Basic Energy Sciences under Grant No. DE-FG02-99ER45761. The collaboration was supported by the U.S. Department of Energy through the Computational Materials and Chemical Sciences Network CM-SCN. Research at Ames Laboratory supported by the U.S. Department of Energy, Office of Basic Energy Sciences, Division of Materials Sciences and Engineering. Ames Laboratory is operated for the U.S. Department of Energy by Iowa State University under Contract No. DE-AC02-07CH11358.

\* Equally contributed to this work

- [1] G. Robert, A. Pasturel, and B. Siberchicot, *J. Phys. Condens. Matter* **15**, 8377 (2003).
- [2] P. Söderlind and B. Sadigh, *Phys. Rev. Lett.* **92**, 185702 (2004).
- [3] A. L. Kutepov and S. G. Kutepova, *J. Magn. Magn. Mater.* **272276**, e329 (2004).
- [4] P. Söderlind, A. Landa, J. E. Klepeis, Y. Suzuki, and A. Migliori, *Phys. Rev. B* **81**, 224110 (2010).
- [5] J. C. Lashley, A. Lawson, R. J. McQueeney, and G. H. Lander, *Phys. Rev. B* **72**, 054416 (2005).
- [6] S. Savrasov, G. Kotliar, and E. Abrahams, *Nature* **410**, 793 (2001).
- [7] J. H. Shim, K. Haule, and G. Kotliar, *Nature* **446**, 513 (2007).
- [8] L. V. Pourovskii, G. Kotliar, M. I. Katsnelson, and A. I. Lichtenstein, *Phys. Rev. B* **75**, 235107 (2007).
- [9] C. A. Marianetti, K. Haule, G. Kotliar, and M. J. Fluss, *Phys. Rev. Lett.* **101**, 056403 (2008).
- [10] M. C. Gutzwiller, *Phys. Rev.* **137**, A1726 (1965).
- [11] N. E. Zein, *Phys. Rev. B* **52**, 11813 (1995).
- [12] X. Y. Deng, L. Wang, X. Dai, and Z. Fang, *Phys. Rev. B* **79**, 075114 (2009).
- [13] K. M. Ho, J. Schmalian, and C. Z. Wang, *Phys. Rev. B* **77**, 073101 (2008).
- [14] N. Lanatà, H. U. R. Strand, X. Dai, and B. Hellsing, *Phys. Rev. B* **85**, 035133 (2012).
- [15] N. Lanatà, Y. X. Yao, C. Z. Wang, K. M. Ho, and G. Kotliar (2014), cond-mat/1405.6934.
- [16] S. Dabos-Seignou, J. Dancausse, E. Gering, S. Heathman, and U. Benedict, *Journal of Alloys and Compounds* **190**, 237 (1993), ISSN 0925-8388.
- [17] P. W. Bridgman, *Journal of Applied Physics* **30**, 214 (1959).
- [18] P. Faure and C. Genestier, *Journal of Nuclear Materials* **385**, 38 (2009), ISSN 0022-3115.
- [19] P. Söderlind, A. Landa, J. E. Klepeis, Y. Suzuki, and A. Migliori, *Phys. Rev. B* **81**, 224110 (2010).
- [20] D. C. Wallace, *Phys. Rev. B* **58**, 15433 (1998).
- [21] W. H. Zachariasen and F. H. Ellinger, *Acta Cryst.* **16**, 369 (1963).
- [22] C. H. Booth, Y. Jiang, D. L. Wang, J. N. Mitchell, P. H. Tobash, E. D. Bauer, M. A. Wall, P. G. Allen, D. Sokaras, D. Nordlund, et al., *Proc. Nat. Acad. Sci.* **109**, 10205 (2012).
- [23] G. van der Laan, K. T. Moore, J. G. Tobin, B. W. Chung, M. A. Wall, and A. J. Schwartz, *Phys. Rev. Lett.* **93**, 097401 (2004).
- [24] K. T. Moore, G. van der Laan, R. G. Haire, M. A. Wall,

- and A. J. Schwartz, Phys. Rev. B **73**, 033109 (2006).
- [25] B. T. Thole and G. van der Laan, Phys. Rev. A **38**, 1943 (1988).
- [26] J. H. Shim, K. Haule, and G. Kotliar, Europhysics Letters **85**, 17007 (2008).
- [27] G. van der Laan and B. T. Thole, Phys. Rev. Lett. **60**, 1977 (1988).
- [28] B. T. Thole and G. van der Laan, Phys. Rev. B **38**, 3158 (1988).
- [29] B. T. Thole and G. van der Laan, Phys. Rev. A **38**, 1943 (1988).
- [30] G. van der Laan and B. T. Thole, Phys. Rev. B **53**, 14458 (1996).
- [31] N. Lanatà, H. U. R. Strand, Y. X. Yao, and G. Kotliar (2013), cond-mat/1310.7520.
- [32] J. X. Zhu, R. Albers, K. Haule, G. Kotliar, and J. Wills, Nat. Commun. **4:2644** (2013).
- [33] C. M. Varma, Rev. Mod. Phys. **48**, 219 (1976).
- [34] P. Blaha, K. Schwarz, G. Madsen, D. Kvasnicka, and J. Luitz, an augmented plane wave plus local orbitals program for calculating crystal properties. University of Technology, Vienna (2001).
- [35] K. Haule, C.-H. Yee, and K. Kim, Phys. Rev. B **81**, 195107 (2010).